

Dynamic slant shear bond behavior between new and old concrete

Bo Hu^{a,*}, Yuan Li^a, Yan Liu^b

^a College of Civil Engineering, Hefei University of Technology, Hefei 230009, PR China

^b Hefei Hengjia Mechanical and Electrical Equipment Company Limited, Hefei 230601, PR China

HIGHLIGHTS

- The strain rate has significant effects on slant shear bond behavior of interfaces.
- The extent of damage of a specimen is related to energy absorbed by the specimen.
- The slant angle affects failure modes and bond strength of specimens.

ARTICLE INFO

Article history:

Received 11 October 2019

Received in revised form 29 November 2019

Accepted 1 December 2019

Keywords:

New-to-old concrete interface

Slant shear test

Strain-rate effect

Bond strength

Energy absorption capacity

ABSTRACT

Quasi-static slant shear bond behavior of new-to-old concrete interfaces has been extensively studied. However, the interfaces might be subjected to dynamic loading during their service life. Therefore, this paper presents an experimental investigation to assess dynamic slant shear bond behavior between new and old concrete. The split Hopkinson pressure bar (SHPB) was employed to apply dynamic compressive loads to slant shear specimens. Quasi-static slant shear tests were also conducted for the purpose of comparison. Test results show that the strain rate has significant effects on failure modes, bond strength, absorption energy and interfacial cohesion and friction angles of specimens. The energy absorption capacity of a specimen in the quasi-static test can be regarded as the threshold in the SHPB test, beyond which the specimen is damaged. Failure modes and bond strength of specimens are influenced by the slant angle but not by the surface roughness and the age of interfaces.

© 2019 Elsevier Ltd. All rights reserved.

1. Introduction

In a concrete structure, concrete is commonly cast at different time, due to limited formworks, the use of post-poured concrete strips, the use of cast-in-situ concrete for connecting precast concrete elements and/or the use of newly added concrete layers for strengthening and repairing existing concrete members. This results in interfaces between new and old concrete, which are usually referred to as weak links in concrete structures [1,2].

For a new-to-old concrete interface, one concern is its bond performance under a state of shear stress that is commonly found in structures and might lead to cracking or even failure of the interface. Commonly used methods to test shear bond behavior between new and old concrete include direct shear [1], bi-surface shear [3,4], push-off [5,6] and slant shear tests [2,3,7–19]. In the first three tests, the interface is actually subjected to both shear and bending stress states during loading. Some stress concentration is induced at the edge of the interface when the shear force

is transmitted using a steel plate. The stress concentration might lead to greater scatter in test results. The slant shear test uses a cylinder or prism sample, which is composed of two identical halves with a certain inclination angle and tested under axial compression. Although the interface is subjected to both shear and compressive stress states during loading, the stress distribution is relatively uniform at the interface. Moreover, slight misalignment of the two halves does not have significant effects on the results. Therefore, the slant shear test has become the most widely adopted test to evaluate shear bond behavior between new and old concrete [2,3,7–19].

Zambas [7] examined effects of the slant angle on bond behavior of new-to-old concrete interfaces. The inclination angle of the interface from vertical was in the range of 10° to 50°. Test results showed that when the slant angle is not greater than 40°, failure occurs along the interface, which is referred to as adhesive failure, and that when the slant angle exceeds 40°, the weakest concrete is crushed, which is regarded as cohesive failure. Cohesive failure leads to a lower estimation for interfacial bond strength. Hence, to accurately obtain bond strength values between new and old concrete, the slant angle of 30° is specified by ASTM standard

* Corresponding author.

E-mail address: bohu@hfut.edu.cn (B. Hu).

C882/C882M-13a [20] and has been employed in most of reported slant shear tests [2,3,8–19]. However, Zanotti et al. [2] and Eymard et al. [8] suggested that the use of a single slant angle of 30° as routinely performed is not sufficient and several slant angles need to be investigated to get a full and rational understanding of interfacial behavior. They tested specimens with three slant angles (i.e., 20°, 25° and 30°) and then determined failure envelopes of the specimen interfaces using the Mohr-Coulomb criterion.

Surface treatment of the old concrete substrate is an important step for preparing a new-to-old concrete interface. Existing tests indicated that commonly used surface treatment methods, including wire-brushing [8–14], sandblasting [11–15], chipping [9,11,12,15], grooving [9,14], hand-chiseling [10], shot blasting [13], hand-scrubbing [13] and acid etching [14], have significant effects on slant shear bond strength of interfaces. It should be noted that when a commonly used surface treatment method is employed, the rough surface is prepared only after the old concrete substrate is cast and demolded. At that time, the old concrete substrate has some strength and hardness. Combined with effects of the strength and skills of operators, the performance of machines and tools and/or the types and dosages of etch agents, in different research and application, the same treatment method might cause different surface roughness and even a lower level treatment method might produce a rougher surface than a higher level treatment method. Thus, there is some uncertainty in the influence of surface roughness on interfacial bond behavior when rough surfaces are generated by commonly used surface treatment methods in research and application. The uncertainty is attributed to that there are no corresponding roughness values or value ranges specified for these treatment methods. In fact, the purpose of surface treatment is to produce surface roughness. The effects of surface treatment methods on interfacial bond behavior are essentially the effects of surface roughness on interfacial bond behavior. Hence, a new concept to eliminate the uncertainty is that the influence of quantitative surface roughness on interfacial bond behavior is firstly investigated, analyzed and determined in research and then one or several appropriate commonly used surface treatment methods are selected to produce the required surface roughness in application. Based on this concept, Saldanha et al. [19] proposed a new surface treatment method for experimental research, by which quantitative interface roughness could be produced with a wavy formwork during the pouring and forming processes of the old concrete substrate. The surface roughness was quantitatively controlled by the height and spacing of waves of the formwork.

Whether or not it is necessary to pre-wet the surface of the old concrete substrate before casting new concrete remains controversial. Júlio et al.'s test results [11] showed that the pre-wetting has insignificant effects on slant shear bond strength. Bentz et al. [15] recommended a dry surface for the old concrete substrate. Their reason was that the compaction of particles on the dry substrate surface might increase frictional resistance. Nevertheless, Chinese code JGJ 1-2014 [21] suggests to pre-wet surfaces of precast (old) concrete elements before applying cast-in-situ (new) concrete. The aim is to prevent dry old concrete substrates absorbing too much water from new concrete. Besides, pre-wetting the substrate surface needs special care when interfacial bonding agents are used, especially epoxy resin, latex and other polymer-based adhesives. It was experimentally found that the effective properties of polymer-based adhesives decrease in the presence of water [22–24]. This is because water molecules, which are polar molecules, can easily penetrate into polymer-based adhesives and lead to plasticization of the adhesives [22].

Diab et al. [9], Júlio et al. [12] and He et al. [17] employed bonding agents to connect new and old concrete. Slant shear test results [9,12,17] indicated that the use of bonding agents can significantly improve bond strength of new-to-old concrete interfaces and the

improvement depends on the properties of bonding agents. However, Júlio et al. [12] also found that the use of bonding agents cannot enhance bond strength if the adopted surface treatment has adequately increased surface roughness.

Concrete has different shrinkage, strength and stiffness at different ages, which might affect bond behavior of new-to-old concrete interfaces. Consequently, Diab et al. [9], Mirmoghtadaei et al. [14] and He et al. [17] examined effects of the age of interfaces on slant shear bond strength. In Diab et al.'s [9] and He et al.'s [17] studies, the testing ages of interfaces were 7 and 28 days, while in Mirmoghtadaei et al.'s [14] study, the testing ages of interfaces were 7, 28 and 90 days. Test results showed that bond strength increases with the increase in the age of interfaces. On the other hand, Santos and Júlio [13] experimentally investigated the influence of the age difference between new and old concrete on slant shear bond strength. Three age differences, i.e., 28, 56 and 84 days, were considered. Specimens were tested when the age of new concrete layers reached 28 days. Test results indicated that bond strength also increases with the increase in the age difference between new and old concrete.

In addition, Diab et al. [9] and Júlio et al. [18] conducted slant shear tests to evaluate effects of compressive strength of new concrete on bond strength. In Diab et al.'s test [9], compressive strength of old concrete was 25 MPa. They found that the improvement of bond strength is pronounced when compressive strength of added self-compacted (new) concrete increases from 25 MPa to 35 MPa, whereas the improvement is limited when the compressive strength is more than 35 MPa. In Júlio et al.'s test [18], compressive strength of old concrete was 30 MPa, while new concrete had compressive strength of 30, 50 and 100 MPa. Test results showed that bond strength increases with the increase in compressive strength of new concrete.

So far, all the reported slant shear tests were focused on bond behavior of new-to-old concrete interfaces under quasi-static loading. Nevertheless, the interfaces might be subjected to dynamic loading during their service life, such as earthquake, blast and vehicle/ship impact. There is a lack of knowledge of dynamic bond behavior between new and old concrete. This paper aims to fill this knowledge gap. A total of 95 slant shear specimens were examined. The split Hopkinson pressure bar (SHPB), which has been widely used to test dynamic behavior of concrete-like materials [25–27], was employed to apply dynamic compressive loads to slant shear specimens. For the purpose of comparison, quasi-static slant shear tests were also carried out. Parameters varied in the tests included the strain rate, the slant angle, the surface roughness and the age of interfaces.

2. Experimental program

2.1. Specimen design

A total of 95 slant shear cylinders were designed, prepared and tested in this experimental program. To investigate effects of the strain rate on bond behavior of new-to-old concrete interfaces, specimens were subjected to four loading rates, including one quasi-static loading rate and three dynamic loading rates. Under the quasi-static loading rate, 23 slant shear specimens were tested, while under each dynamic loading rate, 24 slant shear specimens were tested.

Chinese code JGJ 1-2014 [21] specifies that the strength grade of precast concrete should not be less than the C30 grade and the strength grade of cast-in-site concrete should not be less than that of precast concrete. Chinese code GB 50367-2013 [28] stipulates that newly added concrete for the strengthening and repair of concrete structures should have a higher strength grade than existing

dimension [17]. The surface roughness index is defined by spreading 50 g microsilica sand (50–100 μm) onto the interface, making a circle and measuring its average diameter. This parameter has strict requirements for the material used. The fractal dimension is a measure to describe the overall corrugation and local irregularity of the bonded surface using the fractal geometry theory. The fractal dimension can accurately evaluate the roughness of the entire interface. However, the determination process of this parameter is complicated. The average valley depth is measured using the sand replacement method and calculated by dividing the volume of the sand used to fill the rough surface by the area of the inclined section. The comparative study [30] revealed that the average depth and the fractal dimension have a good linear correlation. It means that the average depth has similar accuracy with the fractal dimension for estimating surface roughness. Moreover, the average depth is more simple and practical than the fractal dimension. Therefore, the average valley depth was employed as the three-dimensional roughness parameter to design the widths and spacing of the rectangular grooves. In this test program, due to the regular interface, the average valley depth was calculated by dividing the volume of the rectangular grooves by the area of the inclined section. To make specimens with different slant angles and the same maximum valley depth have the same average valley depth, the rectangular grooves with widths of 16 and 14 mm and spacing of 14 mm were designed for specimens with the slant angle of 30° and the rectangular grooves with width of 17.5 mm and spacing of 12 mm were designed for specimens with the slant angle of 40° , as shown in Fig. 1. Thus, specimens had two average valley depths, i.e., 1.2 and 2.4 mm. For specimens with different slant angles but the same maximum and average valley depths, the interfaces had unlike texture. However, the interfaces could be considered to have the same surface roughness since they had the same maximum and average valley depths.

Effects of the early age of interfaces on slant shear bond behavior between new and old concrete have been reported in [9,14,17]. However, dynamic loading is more likely to occur during the service life of interfaces. At that time, the age of interfaces is beyond 28 days. Thus, two ages of interfaces, i.e., 60 and 120 days, were used for slant shear specimens in this test program. It should be noted that the age of interfaces was the age of the interfacial zones and it was the same as that of the new concrete layers in this test program.

The identification of specimens is presented in Table 1. "SL" represents the slant shear test. After that, "30" and "40" correspond to slant angles. The following "R1" and "R2" represent the surface roughness and correspond to average valley depths of 1.2 and 2.4 mm, respectively. Then, "A1" and "A2" correspond to interface ages of 60 and 120 days, respectively. Finally, "S" denotes the quasi-static loading rate of 0.2 kN/s, while "V1", "V2" and "V3" correspond to dynamic loading rates of 10.79, 14.70 and 18.19 m/s, respectively.

2.2. Materials

In accordance with Chinese specification JGJ 55-2011 [31], P.O 42.5 Portland cement, medium-sized river sand, coarse aggregate with a maximum gravel size of 10 mm, Type I fly ash, S95 slag powder and potable water were used to fabricate old and new concrete. Besides, two chemical admixtures, i.e., PY-I pumping admixture (6.74 kg/m³) and PCA®-I polycarboxylate superplasticizer (7.92 kg/m³), were adopted for old and new concrete, respectively. Mix proportions of old and new concrete are presented in Table 2. Water-cementitious-material ratios were 0.48 and 0.36 for old and new concrete, respectively.

Compressive strength of cubic samples (150 × 150 × 150 mm³) of old and new concrete was measured when the age of interfaces

reached 60 and 120 days. An average value, corresponding to three concrete samples, was considered for each concrete type and age, as listed in Table 2.

2.3. Specimen preparation

Before casting concrete, formworks needed to be fabricated. PVC tubes with an internal diameter of 70.4 mm and PVC plates with thicknesses of 3 and 6 mm were used for the preparation of formworks. First, a wire-cutting technique was employed to cut PVC tubes and plates to required inclination angles and dimensions. Then, a cyanoacrylate adhesive was used to glue the pre-cut PVC tubes and plates. After that, formworks for twice casting were prepared. The formwork for the first casting, used to form an old concrete substrate and produce a rough surface, was comprised of one tube with an inclined end and one inclined plate with a row of strips, as shown in Fig. 2(a). The strips were cut from the PVC plates and had the same widths and spacing as the designed rectangular grooves. The formwork for the second casting, used to hold the old concrete substrate and form a new concrete layer and a slant shear specimen, consisted of one tube, as shown in Fig. 2(b). It should be noted that the formworks for the first and second casting were 15 and 30 mm higher than the designed specimens, respectively. This was done for the later cutting and grinding of specimens.

C30 concrete was first cast to form old concrete substrates. The substrates were removed from the formworks for the first casting after 24 h and left in the laboratory for 29 days, as shown in Fig. 2(c). Before casting new concrete, surfaces of old concrete substrates were cleaned from any extra particles and dust using compressed air. Afterwards, the surfaces were pre-wetted with water. Then, the old concrete substrates were inserted into the bottom halves of the formworks for the second casting. After that, C40 concrete was cast into the top halves of the formworks. Two days later, slant shear specimens were removed from the formworks and placed in the laboratory.

After 28 days, extra concrete at both ends of the specimen, which was beyond the designed length, was cut off. Then, both ends of the specimen were grinded, so that the non-parallelism of both ends was not more than 0.01 mm. This ensured that both ends of the specimen were in good contact with loading plates in the quasi-static test and pressure bars in the SHPB test. The grinded slant shear specimens are shown in Fig. 2(d).

2.4. Instrumentation and loading procedure

When the age of new-to-old concrete interfaces reached 60 and 120 days, slant shear specimens were tested under quasi-static and dynamic loading. The specimen under quasi-static loading was tested in compression, using a 600 kN universal testing machine (WAW-600), at a constant loading rate of 0.2 kN/s. The quasi-static strain rate of the uniaxial compression test was about 10^{-5} /s. During testing, the compressive load and displacement of the specimen were simultaneously recorded. The test was continued until failure of the specimen. Fig. 3(a) depicts the quasi-static test setup. For consistency, the new concrete layer and the old concrete substrate of each specimen were contacted with the upper and lower loading plates, respectively.

The specimen under dynamic loading was tested on a variable cross-section SHPB apparatus, as shown in Fig. 3(b). The SHPB apparatus includes a striker bar, a variable cross-section incident bar, a transmission bar, an absorption bar and a data acquisition system. Diameters and lengths of the striker, incident and transmission bars are shown in Fig. 3(c). The bars are made of alloy steel with Young's modulus of 210 GPa, density of 7850 kg/m³ and elastic wave propagation velocity of 5172 m/s. The specimen was

Table 1
Test specimens and failure modes.

Specimen	Number of samples	Slant angle (°)	Average valley depth (mm)	Age of interfaces (days)	Loading rate		Average strain rate (1/s)		Failure modes ^b
					Mean ^a	Mean	Mean ^a	Mean	
SL30R1A1S	3	30	1.2	60	0.2 kN/s	0.2 kN/s	10 ⁻⁵	10 ⁻⁵	M4 (3)
SL30R2A1S	2	30	2.4	60	0.2 kN/s		10 ⁻⁵		M4 (2)
SL30R1A2S	3	30	1.2	120	0.2 kN/s		10 ⁻⁵		M4 (3)
SL30R2A2S	3	30	2.4	120	0.2 kN/s		10 ⁻⁵		M4 (3)
SL40R1A1S	3	40	1.2	60	0.2 kN/s		10 ⁻⁵		M3 (3)
SL40R2A1S	3	40	2.4	60	0.2 kN/s		10 ⁻⁵		M3 (2), M4 (1)
SL40R1A2S	3	40	1.2	120	0.2 kN/s		10 ⁻⁵		M3 (3)
SL40R2A2S	3	40	2.4	120	0.2 kN/s		10 ⁻⁵		M3 (3)
SL30R1A1V1	3	30	1.2	60	10.57 m/s	10.79 m/s	8.15	9.91	M2 (2), M4 (1)
SL30R2A1V1	3	30	2.4	60	10.88 m/s		8.15		M2 (2), M4 (1)
SL30R1A2V1	3	30	1.2	120	10.63 m/s		10.13		M1 (2), M2 (1)
SL30R2A2V1	3	30	2.4	120	10.87 m/s		11.97		M1 (1), M2 (2)
SL40R1A1V1	3	40	1.2	60	11.00 m/s		8.57		M1 (2), M2 (1)
SL40R2A1V1	3	40	2.4	60	11.47 m/s		9.87		M1 (3)
SL40R1A2V1	3	40	1.2	120	10.56 m/s		10.97		M1 (3)
SL40R2A2V1	3	40	2.4	120	10.38 m/s		11.50		M1 (3)
SL30R1A1V2	3	30	1.2	60	15.10 m/s	14.70 m/s	17.28	17.05	M3 (1), M4 (2)
SL30R2A1V2	3	30	2.4	60	14.84 m/s		18.10		M4 (3)
SL30R1A2V2	3	30	1.2	120	14.60 m/s		17.80		M4 (3)
SL30R2A2V2	3	30	2.4	120	14.81 m/s		17.77		M4 (3)
SL40R1A1V2	3	40	1.2	60	14.32 m/s		14.99		M1 (1), M2 (1), M3 (1)
SL40R2A1V2	3	40	2.4	60	14.62 m/s		16.45		M1 (1), M3 (1), M4 (1)
SL40R1A2V2	3	40	1.2	120	14.61 m/s		17.73		M3 (3)
SL40R2A2V2	3	40	2.4	120	14.68 m/s		16.27		M3 (3)
SL30R1A1V3	3	30	1.2	60	18.14 m/s	18.19 m/s	20.34	21.63	M4 (3)
SL30R2A1V3	3	30	2.4	60	18.30 m/s		23.43		M4 (3)
SL30R1A2V3	3	30	1.2	120	18.26 m/s		23.00		M3 (1), M4 (2)
SL30R2A2V3	3	30	2.4	120	18.21 m/s		22.73		M4 (3)
SL40R1A1V3	3	40	1.2	60	18.15 m/s		22.61		M5 (3)
SL40R2A1V3	3	40	2.4	60	18.37 m/s		20.71		M5 (3)
SL40R1A2V3	3	40	1.2	120	18.04 m/s		19.60		M5 (3)
SL40R2A2V3	3	40	2.4	120	18.07 m/s		20.60		M5 (3)

^a Note: The mean value corresponds to two or three samples with the same characteristics.

^b The number in parentheses denotes the number of specimens in which the same failure mode occurs.

Table 2
Mix proportions and compressive strength of concrete.

Type	Grade	Mix proportion (kg/m ³)							Compressive strength (MPa)	
		Cement	River sand	Coarse aggregate	Fly ash	Slag powder	Water	Chemical admixture	A1	A2
Old concrete	C30	345	732	970	34	42	202	6.74	55.2 (90 days)	56.0 (150 days)
New concrete	C40	407	655	983	42	79	190	7.92	61.9 (60 days)	62.8 (120 days)

sandwiched between the incident and transmission bars. For consistency, the new concrete layer and the old concrete substrate of each specimen were contacted with the incident and transmission bars, respectively. Before that, the end surfaces of the specimen were evenly smeared with a small amount of vaseline to reduce friction between the specimen and the bars. A piece of rubber with diameter of 5 mm and thickness of 1 mm was attached on the top surface of the incident bar. The rubber was used as a pulse shaper to decrease the high frequency oscillation of the pulse generated by collision between the striker bar and the incident bar. The striker bar was launched with compressed air. Strain gauges were mounted on the incident and transmission bars to measure incident, reflected and transmitted strain waves, as shown in Fig. 3 (c). In this test program, three striker impact velocities, i.e., 10.79, 14.70 and 18.19 m/s, were employed as three dynamic loading rates, and corresponding average strain rates were 9.91, 17.05 and 21.63/s, respectively. The average strain rate was calculated by the total strain in the loading process divided by the corresponding time [27].

Based on the theory of one-dimensional stress wave propagation, the stress, $\sigma(t)$, strain rate, $\dot{\epsilon}(t)$, and strain, $\epsilon(t)$, of the specimen in the SHPB test were calculated by the following equations:

$$\sigma(t) = E \left(\frac{A}{A_s} \right) \epsilon_t(t) \tag{1}$$

$$\dot{\epsilon}(t) = \frac{2C_0}{L} (\epsilon_i(t) - \epsilon_t(t)) \tag{2}$$

$$\epsilon(t) = \int_0^T \dot{\epsilon}(t) dt \tag{3}$$

where E , A and C_0 are the Young's modulus, cross sectional area and wave propagation velocity of pressure bars, respectively; A_s and L are the cross sectional area and length of the tested specimen, respectively; and $\epsilon_i(t)$ and $\epsilon_t(t)$ are the measured incident and transmitted strains, respectively.

It should be noted that it is important for a valid SHPB test to achieve the longitudinal stress equilibrium [26,27]. The following expression was used to check the stress equilibrium in SHPB tests,

$$V_i + V_r = V_t \tag{4}$$

where V_i , V_r and V_t are the incident, reflected and transmitted voltage signals, respectively. A typical set of voltage–time histories of a specimen under a striker impact velocity of 14.70 m/s is given in

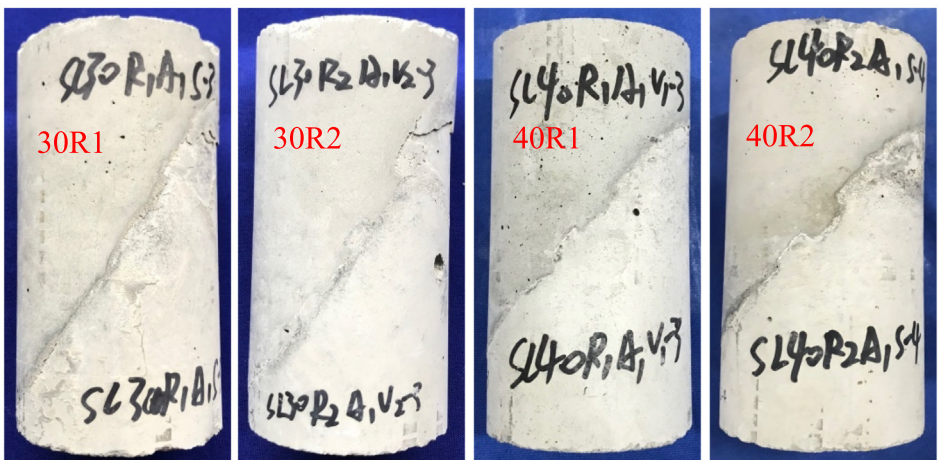


(a)

(b)



(c)



(d)

Fig. 2. Formworks and specimens: (a) formwork for the first casting; (b) formwork for the second casting; (c) old concrete substrates; and (d) slant shear specimens.

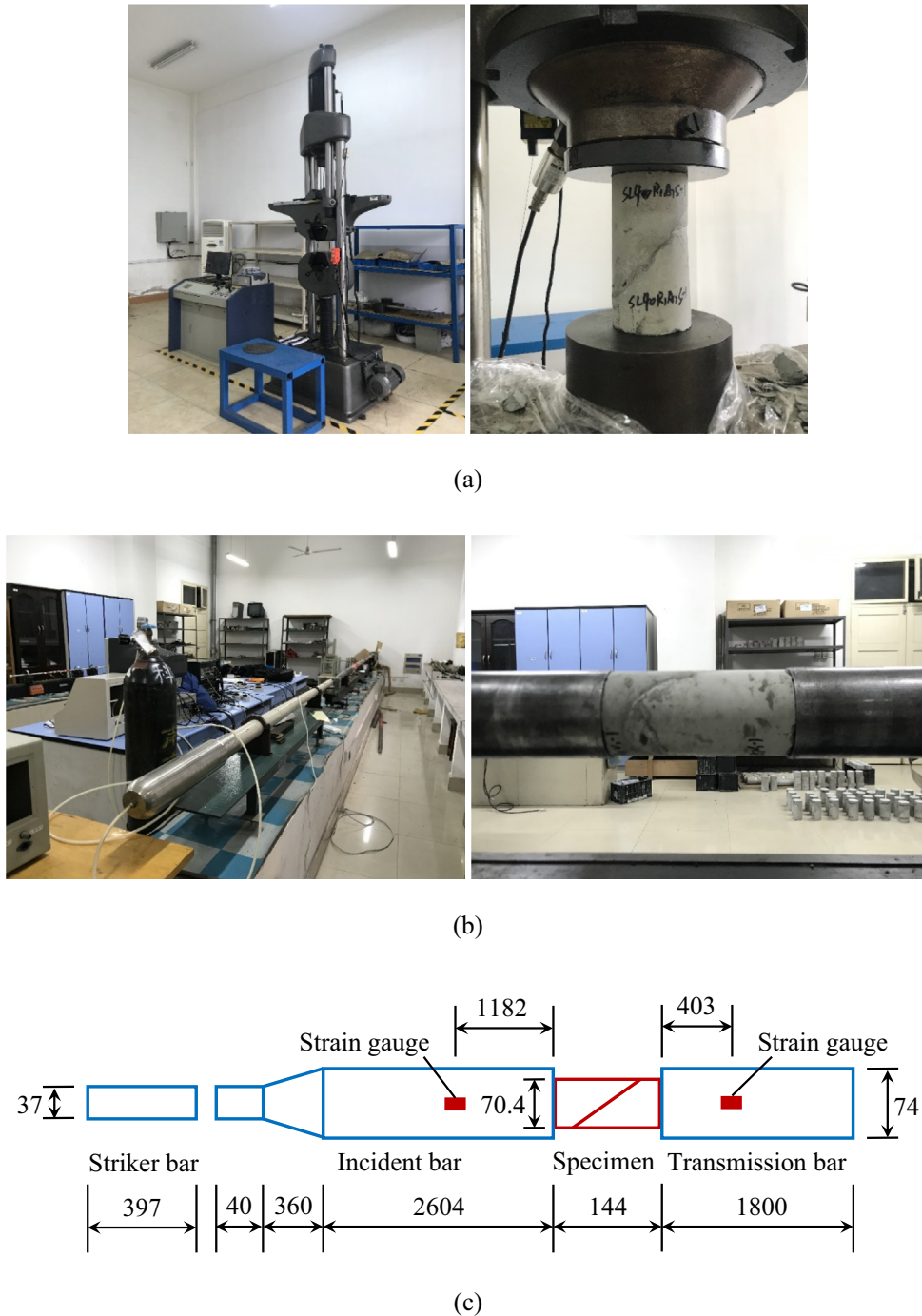


Fig. 3. Test setups and configuration: (a) quasi-static test setup; (b) SHPB test setup; and (c) configuration of the SHPB test (in mm).

Fig. 4. Note that the time lags were removed for clearer comparison. From Fig. 4, it can be seen that the stress equilibrium state was achieved, indicating the validity of SHPB tests presented in this paper.

3. Results and discussion

3.1. Failure modes

According to the extent and characteristics of damage, failure modes of slant shear specimens under quasi-static and dynamic loading can be classified into five typical modes:

- M1—the specimen remains intact, as shown in Fig. 5(a);
- M2—the failure plane passes through a flat portion of the interface and cuts off the tip from the old concrete substrate, as shown in Fig. 5(b);
- M3—the failure plane passes through a flat portion of the interface and splits the old concrete substrate, as shown in Fig. 5(c);
- M4—the failure plane passes through the entire interface and cuts off the bulges from the new concrete layer, i.e., adhesive failure, as shown in Fig. 5(d);
- and M5—the failure plane passes through the entire interface, both the new concrete layer and the old concrete substrate are damaged and the damage of the old concrete substrate is

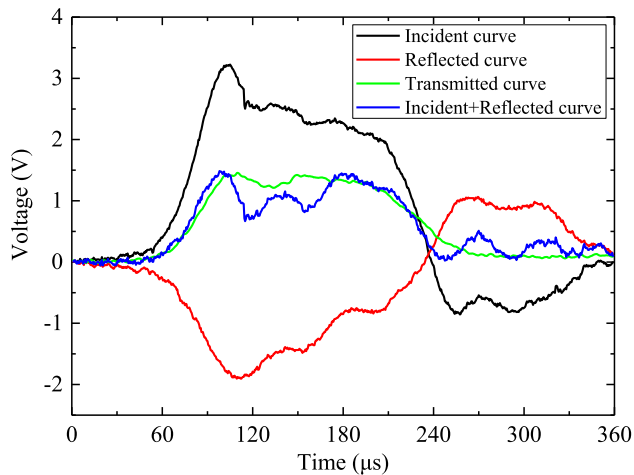


Fig. 4. Stress equilibrium check (SL40R1A2V2).

more serious than that of the new concrete layer, as shown in Fig. 5(e).

Table 1 lists the failure modes of slant shear specimens and the numbers of specimens in which the same failure mode occurs. It is clear from Table 1 that, in quasi-static tests, M4 occurs in all of specimens with the slant angle of 30°, while M3 occurs in most of specimens with the slant angle of 40°. When the average strain rate is 9.91/s, for specimens with the slant angle of 30°, M2 and M4 take place at the interface age of 60 days, while M1 and M2 take place at the interface age of 120 days. It seems to demonstrate that the specimens suffer less damage as the age of interfaces increases. However, specimens with the slant angle of 40° are almost intact and effects of the age of interfaces are not significant. When the average strain rate rises up to 17.05/s, failure modes of specimens are similar to those of specimens in quasi-static tests. That is, M4 happens in most of specimens with the slant angle of 30°, while M3 happens in most of specimens with the slant angle of 40°. Under the average strain rate of 21.63/s, M4 still occurs in most of specimens with the slant angle of 30°, while M5 occurs in all of specimens with the slant angle of 40°.

Test results in Table 1 reveals that the strain rate and the slant angle have significant influence on failure modes of specimens, whereas effects of the surface roughness and the age of interfaces are slight. Interestingly, specimens do not necessarily suffer more damage with the increase in the strain rate. The damage of specimens in quasi-static tests is more serious than that of specimens under the average strain rate of 9.91/s, and similar to that of specimens under the average strain rate of 17.05/s. Regardless of quasi-static or dynamic loading specimens are subjected to, adhesive failure is more likely to happen in specimens with the slant angle of 30° rather than 40°.

3.2. Load-deformation curves in quasi-static tests

Fig. 6 shows axial load-deformation curves of specimens in quasi-static tests. It can be seen from Fig. 6 that, as the axial deformation increases, the axial load of a specimen increases slowly first, and then quickly rises up to the peak value. After that, the axial deformation does not increase anymore and the axial load rapidly drops to the value of 0 MPa. When the age of interfaces increases from 60 days to 120 days, the peak loads of specimens change little, but the ultimate deformation increases. It indicates that axial stiffness of specimens decreases with the increase in the age of interfaces. Unchanged load capacities of specimens

might be attributed to that concrete strength is relatively stable when the concrete age is beyond 28 days. When the average valley depth increases from 1.2 mm to 2.4 mm, the peak loads of specimens with the slant angle of 30° change little, but the ultimate deformation decreases. It might be due to that, when the inclination angle is 30°, higher surface roughness leads to a smaller interfacial slip under the axial load component in the shear direction. The smaller interfacial slip leads to the less ultimate deformation. However, when the inclination angle becomes 40°, the axial load component in the shear direction is lower. The interfacial slip caused by the shear component is slight. Thus, with the increase in the surface roughness, the ultimate deformation is almost unchanged under the same peak loads.

3.3. Stress-strain curves in SHPB tests

According to Eqs. (1) and (3), axial stress and strain values of specimens in SHPB tests can be calculated. Then, the axial stress-strain curves of specimens are obtained, as shown in Fig. 7.

When the average strain rate is 9.91/s, the stress of a specimen increases linearly first with the increase in the strain. Before the stress reaches the peak value, the increase of the stress becomes slower. After the stress exceeds the peak value, a linear elastic unloading begins. It indicates that the specimen separates from pressure bars and undergoes recovery. Finally, the stress-strain curve ends up with slight residual strain. When the age of interfaces is 60 days, the unloading stiffness of specimens is similar to the loading stiffness. When the age of interfaces increases from 60 days to 120 days, the peak stress becomes lower. It is not expected and might be attributed to a variation in the amount of vaseline. A more amount of vaseline caused lower end surface friction, which led to the lower peak stress. Under the same strike impact velocity, the energy absorbed by specimens is almost equal, as presented in section 3.5. Thus, the reduction of the peak stress leads to the improvement of the maximum strain. Moreover, the unloading stiffness becomes smaller with the increase in the age of interfaces. However, the slant angle and the surface roughness have insignificant effects on stress-strain curves of specimens.

Under the average strain rates of 17.05 and 21.63/s, the stress of a specimen also increases linearly with the increase in the strain. Nevertheless, when the stress achieves 40–55 MPa, a transition happens, where the stress increases slowly or does not increase with the increase in the strain. After that, the stress continues to increase linearly. Before the stress reaches the peak value, the increase of the stress becomes more moderate. After the stress exceeds the peak value, the stress decreases with the increase in the strain. When the strain achieves the maximum value, the stress and strain begin to decrease simultaneously and the specimen undergoes recovery. At the end of the stress-strain curve, remarkable residual strain appears. When the average strain rate increases from 9.91/s to 17.05/s, the peak stress increases significantly, but when the average strain rate increases from 17.05/s to 21.63/s, the peak stress increases slightly. When the average strain rate increases from 9.91/s to 21.63/s, the residual strain becomes greater. These indicate that the strain rate has significant effects on stress-strain curves of specimens. When the average strain rate is 17.05/s, the residual strain of specimens with the slant angle of 30° is greater than that of specimens with the slant angle of 40°. It should be attributed to that specimens with the slant angle of 30° undergo more damage and less recovery. Under the average strain rates of 17.05/s, the unloading stiffness is similar to the loading stiffness, while under the average strain rates of 21.63/s, the unloading stiffness is smaller than the loading stiffness. It might be because specimens under the average strain rates of 21.63/s suffer more serious damage and their recovery becomes more difficult. Unlike under the average strain rate of 9.91/s, when



Fig. 5. Typical failure modes of slant shear specimens: (a) M1 (SL40R2A1V1); (b) M2 (SL30R2A1V1); (c) M3 (SL40R1A1V2); (d) M4 (SL30R1A2S); and (e) M5 (SL40R1A1V3).

the average strain rate exceeds 17.05/s, the slant angle, the surface roughness and the age of interfaces have little influence on stress-strain curves of specimens and the strain rate becomes the dominant factor.

3.4. Slant shear bond strength

Fig. 8 describes average measured slant shear bond strength values and corresponding coefficients of variations of specimens at different average strain rates. Note that slant shear bond strength of a specimen is calculated by dividing the load capacity of the specimen at failure by the area of the bonded surface [20].

From Fig. 8, it can be found that slant shear bond strength has significant enhancement when the average strain rate increases from 10^{-5} /s to 9.91/s, but the enhancement becomes slight when the average strain rate exceeds 17.05/s. It reveals that the strain rate has significant effects on slant shear bond strength between new and old concrete. Compared to specimens with the slant angle of 30° , specimens with the slant angle of 40° have higher bond strength at each average strain rate. Under quasi-static loading, higher bond strength of specimens with the slant angle of 40° should be attributed to that the specimens have higher peak loads and smaller bonding areas. Under dynamic loading, the peak loads of specimens with the slant angle of 30° are close to those of specimens with the slant angle of 40° . Thus, smaller bonding areas

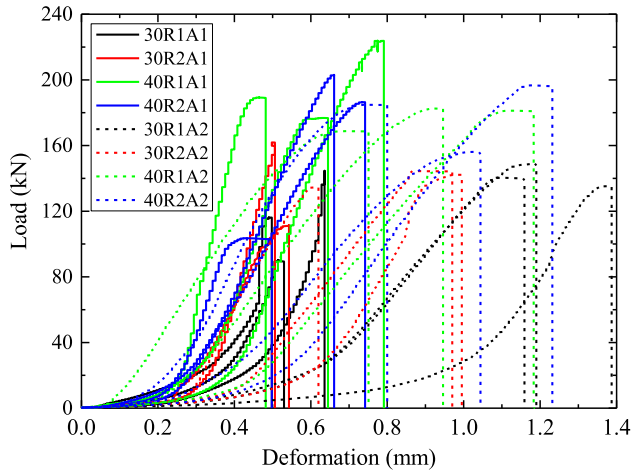


Fig. 6. Load-deformation curves of specimens in quasi-static tests.

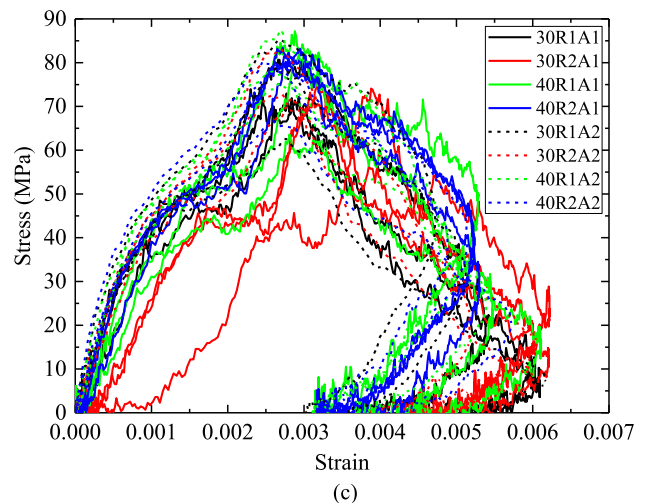
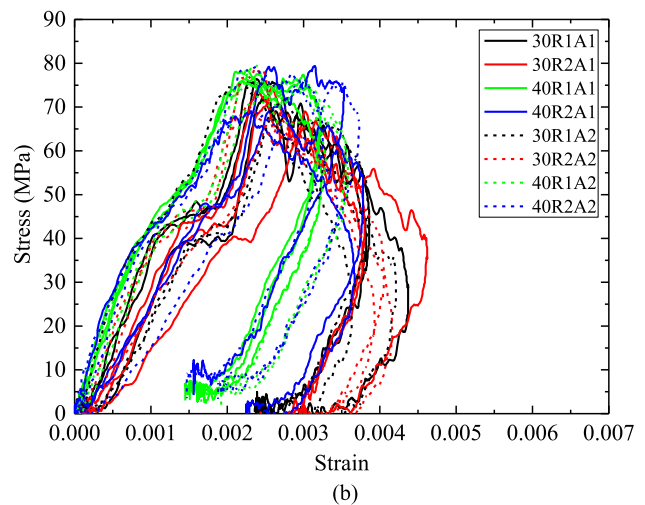
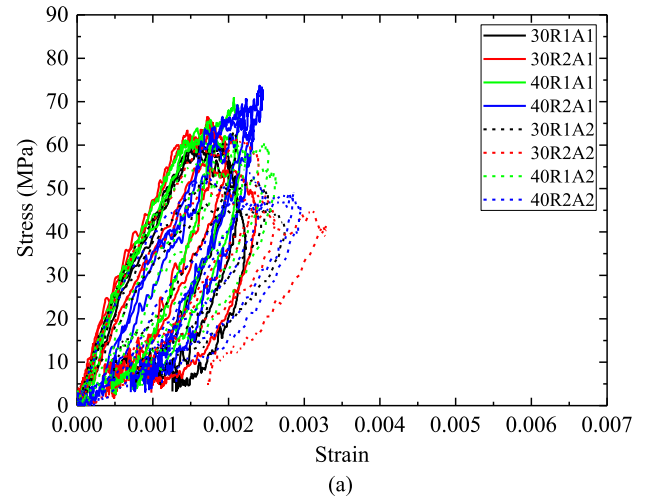


Fig. 7. Stress-strain curves of specimens in SHPB tests: (a) average strain rate of 9.91/s; (b) average strain rate of 17.05/s; and (c) average strain rate of 21.63/s.

become the only factor that leads to higher bond strength of specimens with the slant angle of 40°. Despite there are some fluctuations in results, the age of interfaces has little influence on slant shear bond strength in general. It might be due to that the ages of interfaces in this test program, i.e., 60 and 120 days, are more than 28 days, and at the ages the increase of concrete strength is very limited.

The surface roughness in this test program, i.e., average valley depths of 1.2 and 2.4 mm, also has little effect on slant shear bond strength. In failure mode M1, the specimen is intact, indicating its slant shear bond strength is irrelevant to the surface roughness of the interface. According to failure modes M2, M3, M4 and M5 shown in Fig. 5, two typical interfacial crack patterns are drawn and shown in Fig. 9. In failure modes M2 and M3, the interfacial crack only occurs on a flat portion of the interface, and then the crack switches into the old concrete substrate when it reaches the first rectangular groove. Within this condition, slant shear bond strength depends on interfacial bond strength of the flat portion and compressive strength of the old concrete substrate. For specimens with two average valley depths, old concrete substrates have the same compressive strength. Additionally, the flat portions of the interfaces have the same area and roughness for each inclination angle, as shown in Fig. 1, indicating interfacial bond strength at failure is equal in this crack pattern. These reasons result in little effects of the surface roughness on slant shear bond strength of specimens in which M2 and M3 occur. On the other hand, in failure modes M4 and M5, the interfacial crack occurs on an inclined plane, which has the same inclination angle as the interface and passes through the entire interface. Within this condition, although the new concrete layer and the old concrete substrate have different extent of damage, slant shear bond strength is mainly influenced by interfacial bond strength of the inclined plane. The interfacial crack cuts off all the rectangular bulges from their roots, as shown in Fig. 5(d) and (e). It reveals that interfacial bond strength in this crack pattern is relevant to the width and spacing of the rectangular grooves. In this test program, although the rectangular grooves have two depths, i.e., 3 and 6 mm, they have the same width and spacing for each inclination angle. It should be the reason for little effects of the surface roughness on slant shear bond strength of specimens in which M4 and M5 occur.

3.5. Energy absorption capacities

Fig. 10 presents average absorption energy and corresponding coefficients of variations of specimens at different average strain

rates. In the quasi-static test, the energy absorbed by a specimen is determined by the area under the load-deformation curve shown in Fig. 6. In the SHPB test, the energy absorbed by a specimen is equal to the strain energy multiplied by the specimen volume. The strain energy is determined by the area under the stress-strain curve shown in Fig. 7.

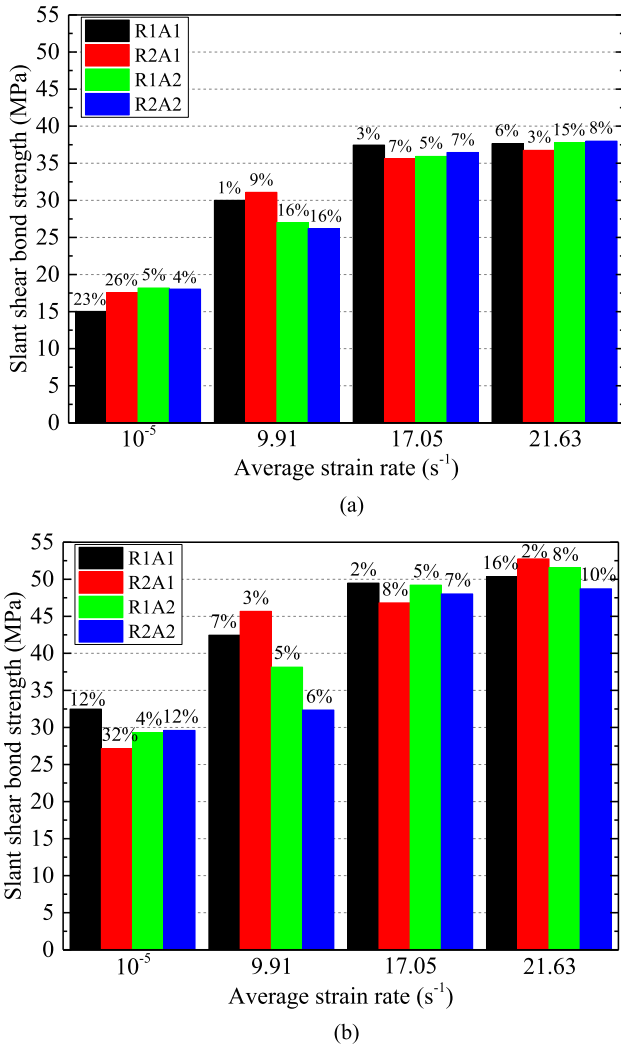


Fig. 8. Slant shear bond strength at different average strain rates: (a) specimens with the slant angle of 30°; and (b) specimens with the slant angle of 40°. (Note: percentages on the tops of the columns represent coefficients of variances of test results.)

Clearly, in quasi-static tests, energy absorption capacities of specimens at the interface age of 120 days are more than those of specimens at the interface age of 60 days. It is due to that specimens at the interface age of 120 days go through more deformation under almost the same loads. When the inclination angle changes from 30° to 40°, specimens absorb more energy. The reason is that specimens with the slant angle of 40° have greater load capacities than those with the slant angle of 30°, as shown in Fig. 6.

In SHPB tests, absorption energy of specimens increases significantly when the average strain rate increases from 9.91/s to 21.63/s. With the increase in the absorption energy, the damage of specimens becomes more serious, as shown in Fig. 5 and Table 1. However, the age of interfaces has little influence on energy absorption capacities of specimens under dynamic loading. When the inclination angle changes from 30° to 40°, energy absorption capacities of specimens decrease under average strain rates of 9.91 and 17.05/s but change little under the average strain rates of 21.63/s. It might be due to that specimens with the slant angle of 30° suffer more damage than those with the slant angle of 40° under average strain rates of 9.91 and 17.05/s, whereas specimens sustain very serious damage under the average strain rate of 21.63/s regardless of 30° or 40° the inclination angle is.

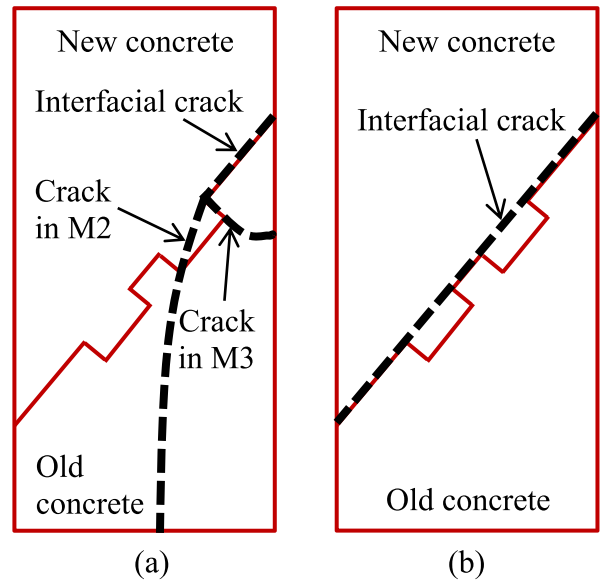


Fig. 9. Two interfacial crack patterns: (a) interfacial crack in M2 and M3; and (b) interfacial crack in M4 and M5.

Interestingly, when the average strain rate increases from 10⁻⁵/s to 9.91/s, absorption energy of specimens does not necessarily increase. For specimens with the slant angle of 30°, the absorption energy under the average strain rate of 9.91/s is greater than that under the average strain rate of 10⁻⁵/s when the age of interfaces is 60 days, whereas the absorption energy under the average strain rate of 9.91/s is lower than that under the average strain rate of 10⁻⁵/s when the age of interfaces is 120 days. For specimens with the slant angle of 40°, the absorption energy under the average strain rate of 9.91/s is smaller than that under the average strain rate of 10⁻⁵/s regardless of 60 or 120 days the age of interfaces is. Even when the age of interfaces is 120 days, the absorption energy under the average strain rate of 17.05/s is almost equal to that under the average strain rate of 10⁻⁵/s. It can be found that a specimen is obviously damaged in the SHPB test when the absorption energy of the specimen under dynamic loading exceeds the energy absorption capacity of the specimen under quasi-static loading, and conversely, the specimen remains intact. It also indicates that the energy absorption capacity of a slant shear specimen under quasi-static loading can be regarded as the threshold under dynamic loading, beyond which the specimen is most likely to be damaged in the SHPB test.

3.6. Interfacial cohesion and friction angles

In a slant shear test, shear stress on the interface is combined with normal compressive stress. Based on the Mohr-Coulomb criterion, the interfacial shear stress has a linear relationship with the normal compressive stress. Two interfacial parameters, namely cohesion and friction angle, are used to determine the linear relationship. Fig. 11 plots shear-normal stress interaction using the experimental values of slant shear bond strength at different loading rates. Note that the slant shear bond strength, obtained for the specimens remaining intact or presenting cohesive failure, is also used in this analysis [13]. In addition, effects of the surface roughness and the age of interfaces are not considered herein due to the effects on slant shear bond strength can be negligible in this test program. Thus, the linear failure envelope of the interfaces at each loading rate can be defined using test slant shear bond strength values of specimens with two slant angles and is shown in Fig. 11.

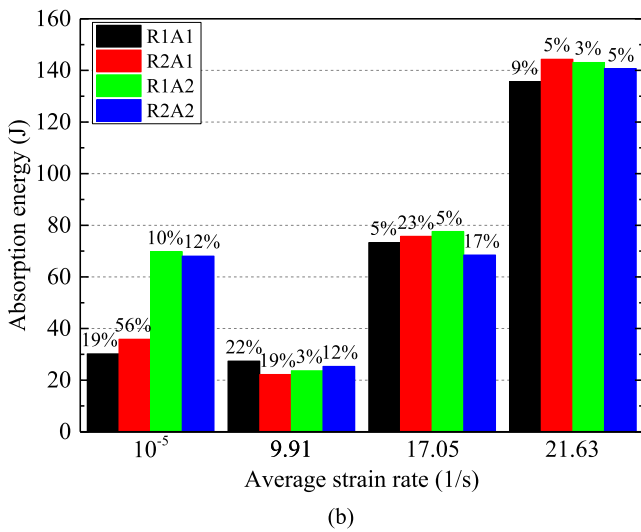
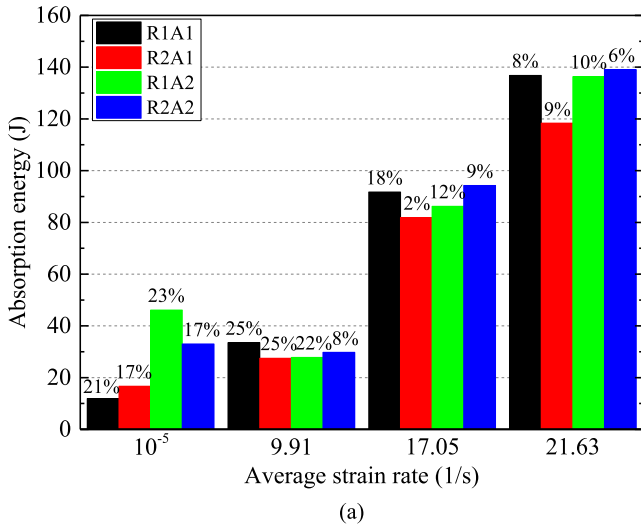


Fig. 10. Absorption energy at different average strain rates: (a) specimens with the slant angle of 30°; and (b) specimens with the slant angle of 40°. (Note: percentages on the tops of the columns represent coefficients of variances of test results.)

Based on linear failure envelopes in Fig. 11, cohesion and friction angles of new-to-old concrete interfaces at different average strain rates are obtained and plotted in Fig. 12(a) and (b), respectively. It can be seen that interfacial cohesion increases with the increase in the strain rate. However, after the average strain rate exceeds 17.05/s, interfacial cohesion nearly reaches a plateau. The interfacial friction angle has a rapid reduction when the average strain rate increases from 10⁻⁵/s to 9.91/s, but changes little when the average strain rate is more than 9.91/s. These indicate that the strain rate has significant effects on interfacial cohesion and friction angles between new and old concrete.

Further, two expressions for predicting the dynamic cohesion, c_d , and the dynamic friction angle, φ_d , of new-to-old concrete interfaces, respectively, can be determined by fitting the test data,

$$\frac{c_d}{c_s} = \left(\frac{\dot{\epsilon}}{10^{-5}} \right)^{0.065} \quad (5)$$

$$\frac{\varphi_d}{\varphi_s} = \left(\frac{\dot{\epsilon}}{10^{-5}} \right)^{-0.028} \quad (6)$$

where c_s and φ_s are the quasi-static cohesion and friction angle of new-to-old concrete interfaces, and can be taken as 8.47 MPa and 36.8°, respectively; and $\dot{\epsilon}$ is the strain rate. The fitting curves of

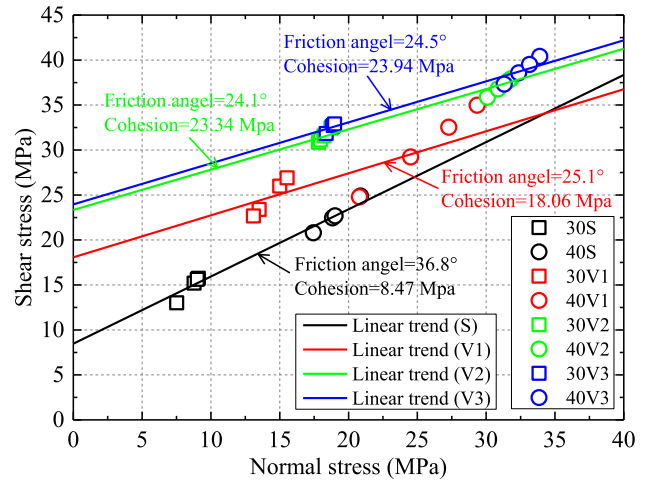


Fig. 11. Experimental shear-normal stress interaction points and linear extrapolations at different loading rates.

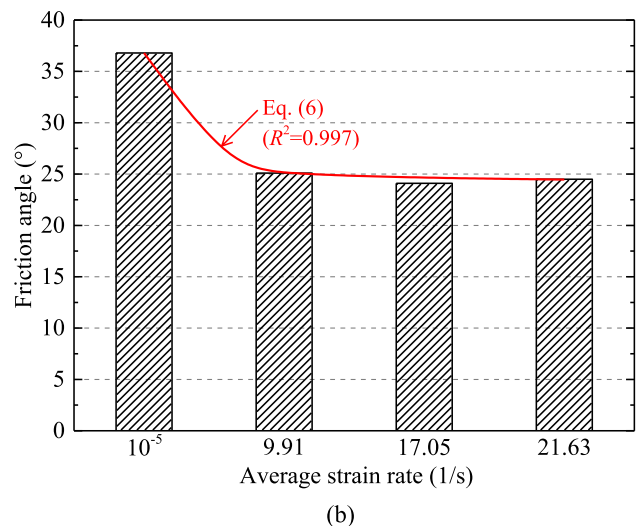
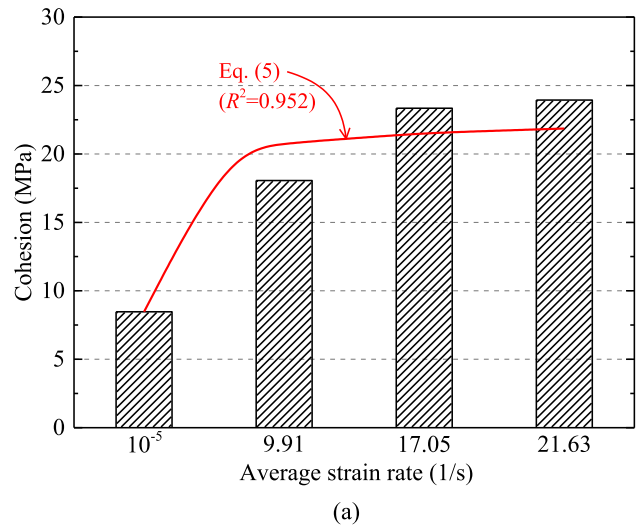


Fig. 12. Interfacial cohesion and friction angles between new and old concrete at different average strain rates: (a) cohesion; and (b) friction angles.

Eqs. (5) and (6) are also shown in Fig. 12(a) and (b), respectively. Coefficients of determination, R^2 , of Eqs. (5) and (6) are 0.952 and 0.997, respectively, indicating the two expressions fit the test data well.

4. Concluding remarks

An experimental program has been carried out to assess slant shear bond behavior of new-to-old concrete interfaces under quasi-static and dynamic loading. Effects of the strain rate, the slant angle, the surface roughness and the age of interfaces on bond behavior have been investigated. Test results include failure modes, load–deformation curves in quasi-static tests, stress–strain curves in SHPB tests, slant shear bond strength, energy absorption capacities and interfacial cohesion and friction angles. The following conclusions are drawn:

- (1) The strain rate has significant effects on failure modes, stress–strain curves, slant shear bond strength, energy absorption capacities and interfacial cohesion and friction angles of specimens. When the average strain rate increases from 10^{-5} /s to 9.91/s, slant shear bond strength and interfacial cohesion significantly increase, but the interfacial friction angle quickly decreases. After the average strain rate exceeds 17.05/s, slant shear bond strength and interfacial cohesion and friction angles change little. Based on the test data, the fitting expressions to determine the dynamic cohesion and friction angle are proposed.
- (2) The energy absorption capacity of a specimen in the quasi-static test can be defined as the threshold in the SHPB test. The specimen in the SHPB test is damaged when its absorption energy is more than the threshold, and conversely, the specimen is intact. When the average strain rate increases from 9.91/s to 21.63/s, specimens absorb more energy and suffer more serious damage.
- (3) Regardless of quasi-static or dynamic loading specimens are subjected to, adhesive failure is more likely to happen in specimens with the slant angle of 30° rather than 40° . When the inclination angle changes from 30° to 40° , slant shear bond strength of specimens increases, while absorption energy of specimens has a reduction under average strain rates of 9.91 and 17.05/s but changes little under the average strain rate of 21.63/s.
- (4) The surface roughness has little influence on slant shear behavior of new-to-old concrete interfaces under quasi-static and dynamic loading. It should be due to that the rectangular grooves on interfaces have the same width and spacing for each inclination angle. Therefore, further works can be focused on effects of the width and spacing of the rectangular grooves.
- (5) Effects of the age of interfaces on failure modes and slant shear bond strength can be ignored because the ages in this test program are more than 28 days. However, with the increase in the age of interfaces, the deformation of specimens in quasi-static tests has significant enhancement. Correspondingly, the absorption energy thresholds in SHPB tests are also raised.

Declaration of Competing Interest

The authors declare that they have no known competing financial interests or personal relationships that could have appeared to influence the work reported in this paper.

Acknowledgments

The financial support of this work from the National Natural Science Foundation of China under Grant No. 51408175 is greatly appreciated. The authors also wish to thank Mr. Dao-Zhong Li from

China Hefei State Construction International Investment and Development Company Limited and Dr. Xu-Tao Wu and Mr. Teng-Fei Meng from Hefei University of Technology for their assistance during the test program.

Appendix A. Supplementary data

Supplementary data to this article can be found online at <https://doi.org/10.1016/j.conbuildmat.2019.117779>.

References

- [1] I. Ray, J.F. Davalos, S. Luo, Interface evaluations of overlay-concrete bi-layer composites by a direct shear test method, *Cem. Concr. Compos.* 27 (3) (2005) 339–347.
- [2] C. Zanotti, N. Banthia, G. Plizzari, A study of some factors affecting bond in cementitious fiber reinforced repairs, *Cem. Concr. Res.* 63 (2014) 117–126.
- [3] A. Momayez, M.R. Ehsani, A.A. Ramezani-pour, H. Rajaie, Comparison of methods for evaluating bond strength between concrete substrate and repair materials, *Cem. Concr. Res.* 35 (4) (2005) 748–757.
- [4] D.S. Santos, P.M.D. Santos, D. Dias-da-Costa, Effect of surface preparation and bonding agent on the concrete-to-concrete interface strength, *Constr. Build. Mater.* 37 (2012) 102–110.
- [5] D. Figueira, C. Sousa, R. Calçada, A.S. Neves, Push-off tests in the study of cyclic behavior of interfaces between concretes cast at different times, *J. Struct. Eng.* 142 (1) (2016) 04015101.
- [6] S.A. Waseem, B. Singh, An experimental study on shear capacity of interfaces in recycled aggregate concrete, *Struct. Concr.* 19 (1) (2018) 230–245.
- [7] C. Zambas, Structural repairs to the monuments of the Acropolis—the Parthenon, *Proc. Inst. Civil Eng. – Civil Eng.* 92 (1992) 166–176.
- [8] M. Eymard, J.P. Plassiard, P. Perrotin, S.L. Fay, Interfacial strength study between a concrete substrate and an innovative sprayed coating, *Constr. Build. Mater.* 79 (2015) 345–356.
- [9] A.M. Diab, A.E.M.A. Elmoaty, M.R.T. Eldin, Slant shear bond strength between self compacting concrete and old concrete, *Constr. Build. Mater.* 130 (2017) 73–82.
- [10] A.I. Abu-Tair, S.R. Rigden, E. Burley, Testing the bond between repair materials and concrete substrate, *ACI Mater. J.* 93 (6) (1996) 553–558.
- [11] E.N.B.S. Júlio, F.A.B. Branco, V.D. Silva, Concrete-to-concrete bond strength. Influence of the roughness of the substrate surface, *Constr. Build. Mater.* 18 (9) (2004) 675–681.
- [12] E.N.B.S. Júlio, F.A.B. Branco, V.D. Silva, Concrete-to-concrete bond strength: influence of an epoxy-based bonding agent on a roughened substrate surface, *Mag. Concr. Res.* 57 (8) (2005) 463–468.
- [13] P.M.D. Santos, E.N.B.S. Júlio, Factors affecting bond between new and old concrete, *ACI Mater. J.* 108 (4) (2011) 449–456.
- [14] R. Mirmoghtadaei, M. Mohammadi, N.A. Samani, S. Mousavi, The impact of surface preparation on the bond strength of repaired concrete by metakaolin containing concrete, *Constr. Build. Mater.* 80 (2015) 76–83.
- [15] D.P. Bentz, I. De la Varga, J.F. Muñoz, R.P. Spragg, B.A. Graybeal, D.S. Hussey, D. L. Jacobson, S.Z. Jones, J.M. LaManna, Influence of substrate moisture state and roughness on interface microstructure and bond strength: slant shear vs. pull-off testing, *Cem. Concr. Compos.* 87 (2018) 63–72.
- [16] P.M.D. Santos, E.N.B.S. Júlio, V.D. Silva, Correlation between concrete-to-concrete bond strength and the roughness of the substrate surface, *Constr. Build. Mater.* 21 (8) (2007) 1688–1695.
- [17] Y. He, X. Zhang, R.D. Hooton, X. Zhang, Effects of interface roughness and interface adhesion on new-to-old concrete bonding, *Constr. Build. Mater.* 151 (2017) 582–590.
- [18] E.N.B.S. Júlio, F.A.B. Branco, V.D. Silva, J.F. Lourenço, Influence of added concrete compressive strength on adhesion to an existing concrete substrate, *Build. Environ.* 41 (12) (2006) 1934–1939.
- [19] R. Saldanha, E. Júlio, D. Dias-da-Costa, P. Santos, A modified slant shear test designed to enforce adhesive failure, *Constr. Build. Mater.* 41 (2013) 673–680.
- [20] ASTM Standard C882/C882M-13a. Standard test method for bond strength of epoxy-resin systems used with concrete by slant shear. ASTM International, West Conshohocken, PA, 2013.
- [21] JGJ 1-2014. Technical specification for precast concrete structures. Ministry of Housing and Urban-Rural Development of the People's Republic of China, Beijing, 2014. (in Chinese)
- [22] M. Mohammadi, R. Mir Moghtadaei, Samani N. Ashraf, Influence of silica fume and metakaolin with two different types of interfacial adhesives on the bond strength of repaired concrete, *Constr. Build. Mater.* 51 (2014) 141–150.
- [23] G.C. Mays, A.R. Hutchinson, Adhesives in civil engineering, Cambridge University Press, Cambridge, 1992.
- [24] M.K. Antoon, M.K. Antoon, J.L. Koenig, Irreversible effects of moisture on the epoxy matrix in glass-reinforced composites, *J. Polym. Sci. – Polym. Phys.* 19 (1981) 197–212.
- [25] M. Zhang, H.J. Wu, Q.M. Li, F.L. Huang, Further investigation on the dynamic compressive strength enhancement of concrete-like materials based on split Hopkinson pressure bar tests. Part I: experiments, *Int. J. Impact. Eng.* 36 (12) (2009) 1327–1334.

- [26] Y. Hao, H. Hao, G.P. Jiang, Y. Zhou, Experimental confirmation of some factors influencing dynamic concrete compressive strengths in high-speed impact tests, *Cem. Concr. Res.* 52 (2013) 63–70.
- [27] T.H. Lv, X.W. Chen, G. Chen, Analysis on the wave form features of the split Hopkinson pressure bar tests of plain concrete specimen, *Int. J. Impact. Eng.* 103 (2017) 107–123.
- [28] GB 50367-2013. Code for design of strengthening concrete structure. Ministry of Housing and Urban-Rural Development of the People's Republic of China, Beijing, 2013. (in Chinese).
- [29] L. Courard, T. Piotrowski, A. Garbacz, Near-to-surface properties affecting bond strength in concrete repair, *Cem. Concr. Compos.* 46 (2014) 73–80.
- [30] Z.F. Zhao, Y.H. Yu, G.F. Zhao, Methods to measuring the interfacial roughness of new-to-old concrete, *Build. Struct.* 30 (1) (2000) 26–29 (in Chinese).
- [31] JGJ 55-2011. Specification for mix proportion design of ordinary concrete. Ministry of Housing and Urban-Rural Development of the People's Republic of China, Beijing, 2011. (in Chinese).